Single production of vectorlike B quarks at the CLIC

Jin-Zhong Han,* Jing Yang, Shuai Xu, and Han-Kui Wang
School of Physics and Telecommunications Engineering, Zhoukou Normal University, Zhoukou 466001, China

(Received 31 August 2021; accepted 22 December 2021; published 6 January 2022)

The vectorlike quarks are predicted in many new physics scenarios beyond the Standard Model (SM) and could be seen potential signatures of new physics at the TeV energy scale. In this work, we study single production of exotic singlet and doublet vectorlike bottom quarks (VLQ-B) at future Compact Linear Collider (CLIC) via the process $e^+e^- \to B\bar{b}$ with the decay channel $B \to bZ$ and two types of modes: $Z \to \ell^+\ell^-$ and $Z \to \nu\bar{\nu}$. We calculate the cross sections of signal and relevant SM backgrounds. After a fast simulation of the signal and background events, the exclusion limit at 95% confidence level and 5σ discovery prospects on the parameters (the coupling strength κ_B and the VLQ-B mass) have been, respectively, presented at the future CLIC with center of mass energy $\sqrt{s} = 3$ TeV and integrated luminosity of 5 ab^{-1}.

DOI: 10.1103/PhysRevD.105.015005

I. INTRODUCTION

In order to solve the gauge hierarchy problem, the vectorlike quarks (VLQs) are predicted to regulate the Higgs boson mass-squared divergence [1] in several extensions of the Standard Model (SM), such as little Higgs models [2], extra dimensions [3], composite Higgs models [4], and other TeV Scale new physics (NP) models [5–8]. The left- and right-handed components of these new VLQs are transformed in the same properties under the SM electroweak symmetry group [9]. The VLQs are therefore not excluded by present searches, unlike a fourth generation of SM quarks that is ruled out by electroweak precision measurements [10,11]. Based on the electric charges of $+2/3e$ (T quark), $-1/3e$ (B quark), $+5/3e$ (X quark) or $-4/3e$ (Y quark), the VLQs could be grouped in multiplets, such as electroweak singlet [T, B], electroweak doublets [(X,T), (T,B) or (B,Y)], or electroweak triplets [(X,T,B) or (T,B,Y)], and they could generate characteristic signatures at the current and future high-energy colliders, see e.g., [12–34]. Here we focus on the singlet or (B,Y) doublet VLQ-B quark, which only couples to third-generation SM quarks.

Using the Run 2 data, the direct searches for VLQ-B have been performed and the constraints on VLQ-B have been obtained at 95% confidence level (CL) by the ATLAS and CMS Collaborations [35–43]. For instance, an analysis from CMS including single-lepton, dilepton, and multilepton final states probed all decay modes of the VLQ-B, and excluded B quark masses in the range 910–1240 GeV [41]. Recently, the CMS Collaboration presented a search for VLQ-B pair production in the fully hadronic final state [42], and excluded the B masses up to 1570, 1390, and 1450 GeV for 100% $B \to bh$, 100% $B \to tZ$, and BY doublet cases, respectively. The combination of searches utilizing various final states were performed by the ATLAS Collaboration [43], and excluded values of the B mass up to 1220, 1370, and 1140 GeV for the singlet, the (T,B) doublet and (B,Y) doublet cases, respectively.

Up to now, many phenomenological analysis about the VLQ-B have been performed at the LHC and LHeC [44–46]. Compared to the complicated QCD background at the hadron colliders, the future linear e^+e^- collider has a particularly clear background environment, i.e., the final stage of Compact Linear Collider (CLIC) are operating at an energy of 3 TeV [47–50]. Thus, the high-energy linear collider is a precision machine that can accurately measure the characteristics of the new VLQs [51–58]. In this work, we focus on the observability of the single VLQ-B production at the CLIC via the process $e^+e^- \to B\bar{b}(b\bar{B})$ combined with the $B \to bZ$ and the subsequent decay channels $Z \to \ell^+\ell^-$ and $Z \to \nu\bar{\nu}$, respectively. The advantage is that it has a higher potential than paired production due to less phase space suppression. In addition, this process can reveal the electroweak nature of the interaction between the VLQ-B and Z boson. Therefore, we expect that once the VLQ-B is discovered and its mass is determined, such work could serve as a complementary option for future high-energy linear colliders.

*hanjinzhong@zknu.edu.cn

The paper is organized as follows. In Sec. II, we give a brief description of the simplified model including the VLQ-B with electrical charge $-1/3$, and discuss its single production at the CLIC. In Sec. III we investigate the signal and discovery potential of the VLQ-B in the Zb decay channel at the CLIC. Finally, we conclude in Sec. IV.

II. VECTORLIKE BOTTOM QUARK IN THE SIMPLIFIED MODEL

The generic parametrization of an effective Lagrangian of VLQ-B can be expressed as (showing only the couplings relevant for our analysis):

$$\mathcal{L} = \kappa_B \left\{ \sqrt{\frac{\zeta_i \xi^B_W}{\Gamma^0_W}} \frac{g}{\sqrt{2}} [\bar{B}_{L/R} W^+_\mu \gamma^\mu u^i_{L/R}] + \sqrt{\frac{\zeta_i \xi^B_Z}{\Gamma^0_Z}} \frac{g}{2c_W} [\bar{B}_{L/R} Z_\mu \gamma^\mu d^i_{L/R}] - \sqrt{\frac{\zeta_i \xi^B_H}{\Gamma^0_H}} \frac{M}{v} [\bar{B}_{R/L} H d^i_{L/R}] \right\} + \text{H.c.}, \quad (1)$$

where g is the $SU(2)_L$ gauge coupling constant, c_W is the usual cosine of the weak mixing angle, $v \simeq 246$ GeV and ξ^V parameters controlling the relative strengths of the V couplings to top partners, and ζ_i parameters governing the mix of SM quark generations i in each coupling. ξ and ζ are defined as $\sum_V \xi^V = 1$ and $\sum_i \zeta_i = 1$, meaning $\zeta_i \xi^V = \mathrm{BR}(B \to V q_i)$ (for a detailed review, see [12]).

Although couplings of VLQs to first- and second-generation SM quarks are not excluded [34,59], much of the experimental and theoretical attention is on VLQs that couple to third-generation SM quarks, as it is this generation that requires fine-tuning in the SM. Here we focus on VLQ-B that couples exclusively to third-generation SM quarks. Our results are interpreted assuming that the B quark belongs to a singlet or doublet representation and that it decays exclusively to SM particles. In this case, the singlet B quark has three different decay channels into SM particles: tW, bZ and bH. Using the equivalence theorem [60–65] the branching fractions for these three decay modes are 0.5, 0.25, and 0.25, respectively. The B doublet can decay to bZ or bH, each with a branching fraction of 0.5. Thus there are only two free parameters: the B quark mass m_B and the coupling strength κ_B.

III. EVENT GENERATION AND DISCOVERY POTENTIALITY

In Fig. 1, we show the leading order Feynman diagram of the process $e^+e^- \to B\bar{b}$ with the decay mode $B \to Zb$.

In order to make a prediction for the signal, we calculate the cross section for the process $e^+e^- \to B\bar{b}(b\bar{B})$ times the branching ratio of $B \to bZ$ at leading order (LO) by using

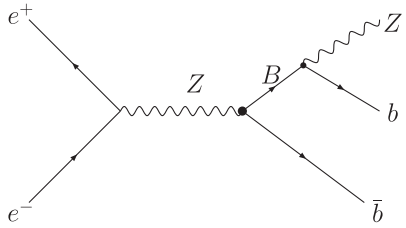

FIG. 1. Representative Feynman diagrams of the process $e^+e^- \to B(\to Zb)\bar{b}$.

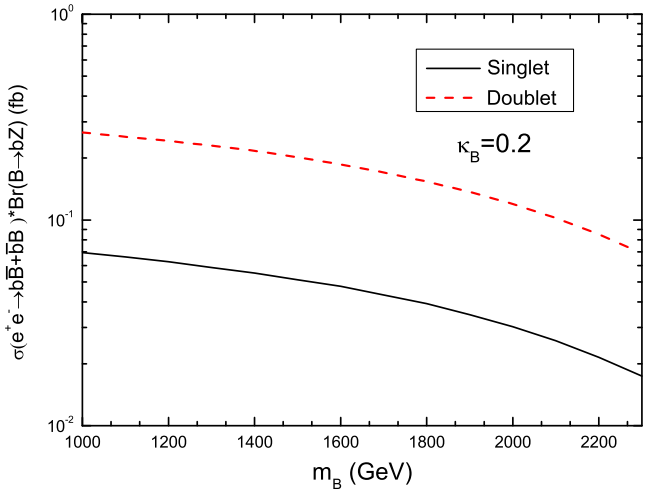

FIG. 2. Total cross sections as a function of m_B with $\kappa_B = 0.2$ and two cases.

MadGraph5-aMC@LO [66]. The numerical values of the input parameters are taken from [67].

In Fig. 2, we show the dependence of the cross sections $\sigma(e^+e^- \to B\bar{b} + b\bar{B}) \times \mathrm{Br}(B \to bZ)$ on the B quark mass m_B at a 3 TeV CLIC for $\kappa_B = 0.2$. As the B quark mass grows, the cross section of single production decreases slowly due to a larger phase space. For $\kappa_B = 0.2$ and $m_B = 1.5(2)$ TeV, the cross section can reach about 0.05 (0.3) fb for the singlet case and 0.2 (0.12) fb for the doublet case, respectively. Obviously, the cross section of single B-quark production is proportional to the square of the coupling strength κ_B for a given B quark mass.

In next section, we will perform the Monte Carlo simulation and explore the discovery potentiality of VLQ-B through the subsequent leptonic decay channel $Z \to \ell^+\ell^-$ and the invisible decay channel $Z \to \nu\bar{\nu}$, respectively.

Monte Carlo event simulations for signal and SM background are interfaced to Pythia 8.20 [68] for fragmentation and showering. All event samples are fed into the Delphes 3.4.2 [69] with the CLIC detector card designed for 3 TeV [70]. In our analysis, jets are clustered with the Valencia Linear Collider (VLC) algorithm [71,72] in exclusive mode with a fixed number of jet ($N = 2$ where N corresponds to the number of partons expected in the

final state) and fixed one size parameter $R = 0.7$. The b-tagging efficiency is taken as the loose working points with 90% b-tagging efficiency in order not to excessively reduce the signal efficiency. The misidentification rates are given as a function of energy and pseudorapidity, i.e., in a bit where $E > 500$ GeV and $1.53 < |\eta| \leq 2.09$, misidentification rates are 5×10^{-2}. Finally, event analysis is performed by using MadAnalysis5 [73].

A. The decay channel $Z \to \ell^+\ell^-$

In this subsection, we analyze the signal and background events at the 3 TeV CLIC through the $Z \to \ell^+\ell^-$ ($\ell = e, \mu$) decay channel.

$$e^+e^- \to B\bar{b} \to Zb\bar{b} \to \ell^+\ell^- b\bar{b}. \tag{2}$$

For this channel, the typical signal is two b-jet and two opposite-sign same-flavor (OSSF) leptons. The dominant SM backgrounds come from the SM processes $e^+e^- \to b\bar{b}\ell^+\ell^-$, and $e^+e^- \to jj\ell^+\ell^-$ with the cross sections of 2.74 fb, and 8.39 fb, respectively. Note that the contribution from the processes $e^+e^- \to H(\to b\bar{b})Z$, $e^+e^- \to Z(\to b\bar{b})Z$, $e^+e^- \to b\bar{b}Z$ and $e^+e^- \to q\bar{q}Z$ are also included with the decay mode $Z \to \ell^+\ell^-$.

To identify objects, we choose the basic cuts at parton level for the signals and SM backgrounds as follows:

$$p_T^{\ell} > 20\,\text{GeV}, \quad p_T^{j/b} > 30\,\text{GeV}, \quad |\eta_{\ell/b/j}| < 2 \tag{3}$$

where $p_T^{\ell,b,j}$ are the transverse momentum of leptons, b-jets, and light jets, respectively.

For the signal, the leptons ℓ_1 and ℓ_2 are two OSSF leptons that are assumed to be the product of the Z-boson decay, and at least two b-tagged jet are present. In Fig. 3, we plot some differential distributions for signals and SM backgrounds at the CLIC, such as the transverse momentum distributions of the leading and subleading b-jets ($p_T^{b_1}, p_T^{b_2}$), the separations $\Delta R_{b_1,b_2}$, the transverse momentum distributions of the leading and subleading leptons ($p_T^{\ell_1\ell_2}$), the separations $\Delta R_{\ell_1,\ell_2}$, and the invariant mass distribution for the Z boson $M_{\ell_1\ell_2}$. Due to the larger mass of VLQ-B, the decay products of VLQ-B are highly boosted. Therefore, the $p_T^{l,b}$ peaks of the signals are larger than those of the SM backgrounds, and the lepton pairs of the signal are much closer. Based on these kinematical distributions, we can impose the following set of cuts:

(i) Cut-1: There are exactly two isolated leptons and two b-tagged jets.
(ii) Cut-2: The transverse momenta of the leading and sub-leading b-jet are required $p_T^{b_1} > 500$ GeV and $p_T^{b_2} > 250$ GeV with $\Delta R_{b_1,b_2} > 1.2$.
(iii) Cut-3: The transverse momenta of the leading and subleading leptons are required $p_T^{l_1 l_2} > 300$ GeV, the invariant mass of the Z boson is required to have $|M_{\ell_1\ell_2} - m_Z| < 10$ GeV with $\Delta R_{\ell_1,\ell_2} < 1$.

We present the cross sections of three typical signal ($m_B = 1300$, 1500, 2000 GeV) and the relevant backgrounds after imposing the cuts in Table I. One can see that all the SM backgrounds are suppressed very efficiently with the cross section of about 0.01 fb, while the signals still have a relatively good efficiency at the end of the cut flow. The total SM background comes from the $e^+e^- \to b\bar{b}\ell^+\ell^-$ process, with a total cross section of 5.34×10^{-3} fb.

B. The decay channel $Z \to \nu\bar{\nu}$

In this subsection, we analyze the signal and background events through the invisible decays $Z \to \nu\bar{\nu}$ decay channel.

$$e^+e^- \to B\bar{b} \to Zb\bar{b} \to b\bar{b} + \not{E}_T. \tag{4}$$

For this channel, the main SM backgrounds come from the processes $e^+e^- \to \nu\bar{\nu}b\bar{b}$ and $e^+e^- \to \nu\bar{\nu}jj$ with the cross sections of 0.26 fb and 0.61 fb, respectively. Note that the contribution from the processes $e^+e^- \to HZ$, $e^+e^- \to \nu_e\bar{\nu}_e H$, $e^+e^- \to \nu_e\bar{\nu}_e Z$, and $e^+e^- \to Zb\bar{b}$ are also included with the decay mode $Z \to \nu\bar{\nu}$ and $H \to b\bar{b}$.

In our simulations, we apply the following basic cuts on the signal and background events at parton level:

$$p_T^{b/j} > 30\ \text{GeV}, \qquad |\eta_{b/j}| < 2, \qquad \not{E}_T > 100\ \text{GeV}. \tag{5}$$

Obviously, the signal events should contain large missing transverse energy $\not{E}_T$ from the boosted Z boson. In order to get some hints of further cuts for reducing the SM backgrounds, we analyzed the normalized distributions of $p_T^{b_1,b_2}$, $p_T^{b_2}$, $\Delta R_{b_1,b_2}$, and $\not{E}_T$ for signals and SM backgrounds as shown in Fig. 4. Based on these kinematical distributions, a set of further cuts are given as:

(i) Cut-1: There are at least two b-tagged jets and remove any electrons and muons.
(ii) Cut-2: The transverse momenta of the leading and subleading b-jet are required $p_T^{b_1} > 300$ GeV and $p_T^{b_2} > 200$ GeV with $\Delta R_{b_1,b_2} > 1.5$.
(iii) Cut-3: The transverse missing energy is required $\not{E}_T > 300$ GeV.

We summarize the cross sections of three typical signal ($m_B = 1300$, 1500, 2000 GeV) and the relevant backgrounds after imposing the cuts in Table II. One can see that the total SM backgrounds are suppressed very efficiently, with a cross section of about 0.1 fb.

C. Discovery and exclusion significance

In order to see whether the signatures of VLQ-B can be detected at the CLIC, we use the median significance to estimate the expected discovery and exclusion significance [74]:

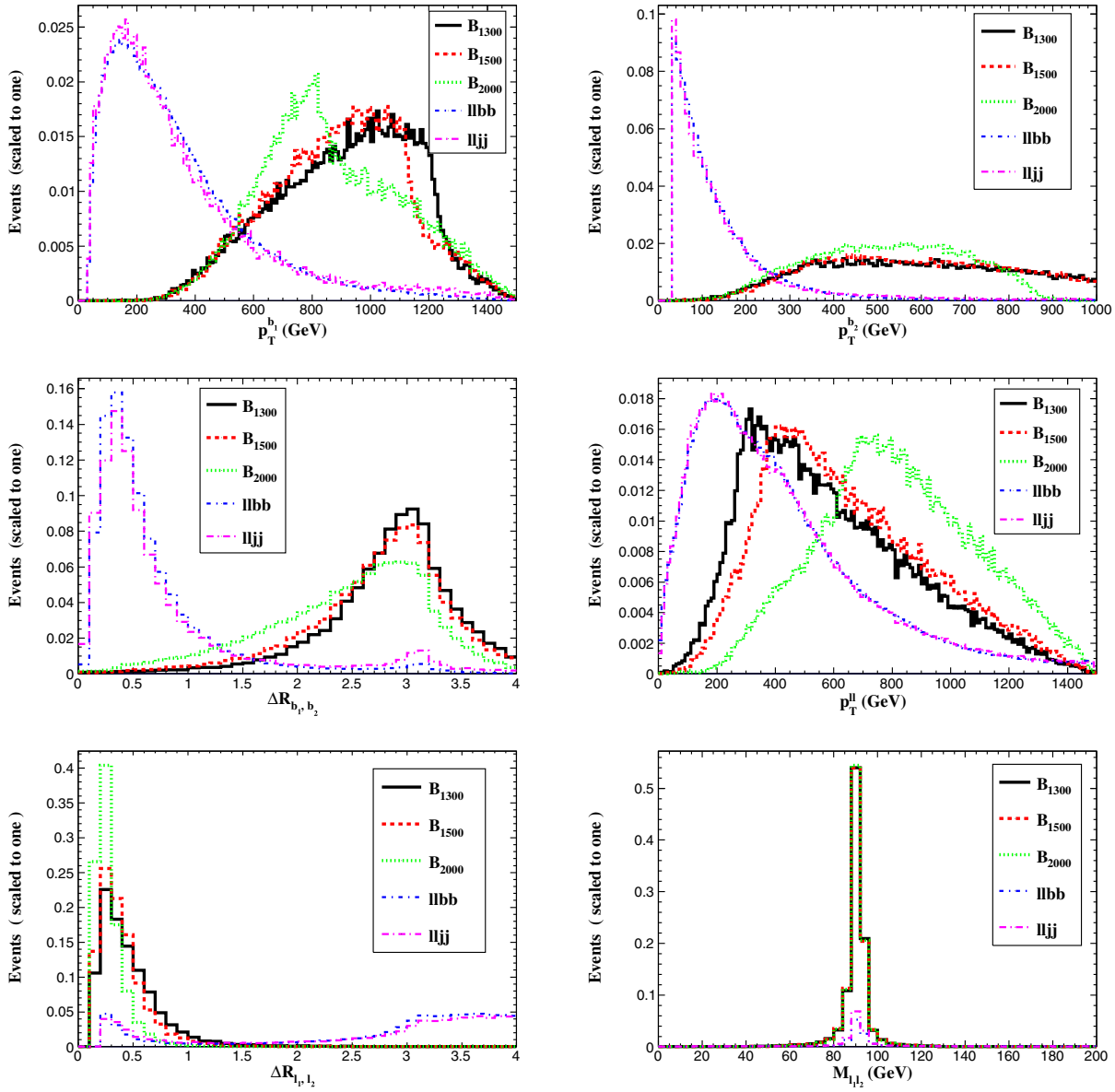

FIG. 3. Normalized distributions for the signals (with $m_B = 1300$, 1500 and 2000 GeV) and SM backgrounds at the CLIC.

TABLE I. Cut flow of the cross sections (in 10^{-3} fb) for the signals and SM backgrounds at the CLIC with $\kappa_B = 0.2$ and three typical B quark masses for the singlet case and doublet case (in the bracket).

	Signals			Backgrounds		
Cuts	1300 GeV	1500 GeV	2000 GeV	$\ell^+\ell^- b\bar{b}$	$\ell^+\ell^- jj$	Total
Basic	3.4 (15.2)	3.3 (13.2)	1.9 (7.6)	1869	1179	3048
Cut 1	2.37 (9.5)	2.1 (8.4)	1.2 (4.8)	689	103	792
Cut 2	2.25 (9.0)	1.95 (7.8)	1.1 (4.4)	18.2	7.7	25.9
Cut 3	1.62 (6.5)	1.58 (6.3)	0.95 (3.8)	5.34	2.02	7.36

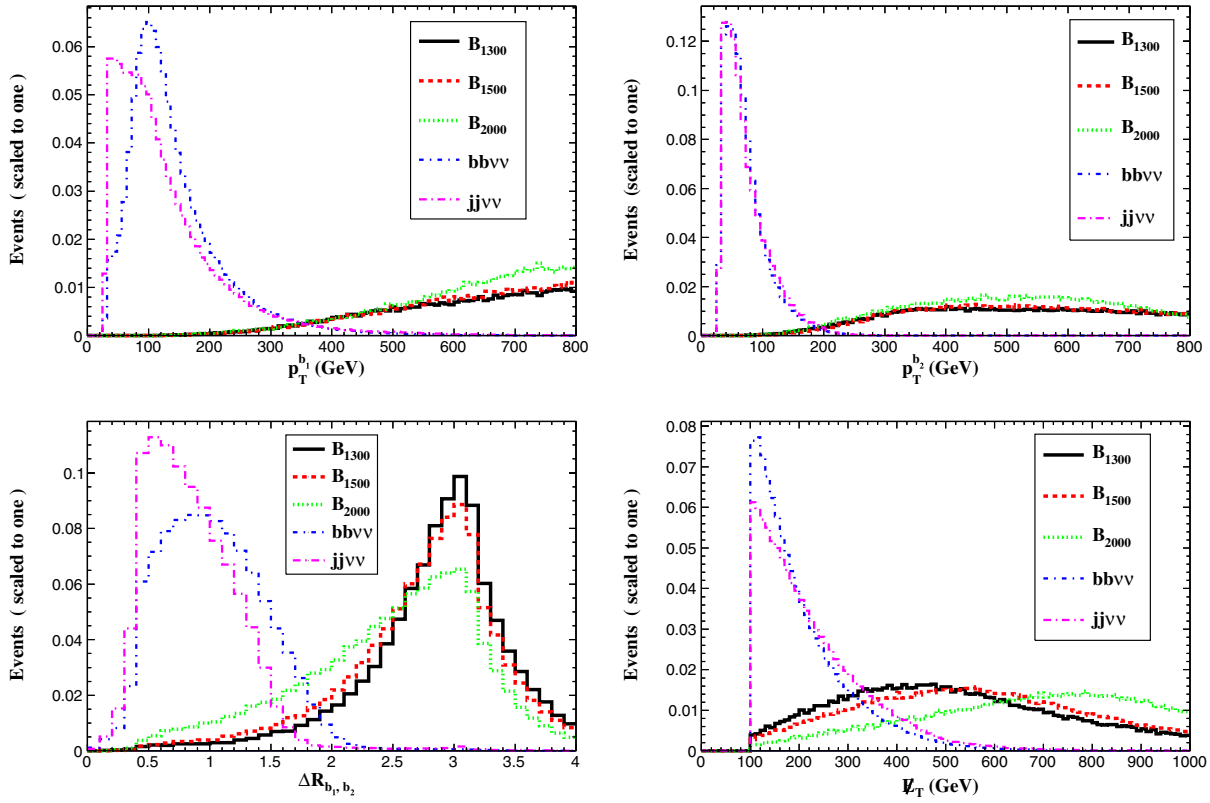

FIG. 4. Normalized distributions for the signals and SM backgrounds for $Z \to \nu\bar{\nu}$ decay channel at the CLIC.

$$\mathcal{Z}_{\text{disc}} = \sqrt{2\left[(s+b)\ln\left(\frac{(s+b)(1+\delta^2 b)}{b+\delta^2 b(s+b)}\right) - \frac{1}{\delta^2}\ln\left(1+\delta^2\frac{s}{1+\delta^2 b}\right)\right]}$$
$$\mathcal{Z}_{\text{excl}} = \sqrt{2\left[s - b\ln\left(\frac{b+s+x}{2b}\right) - \frac{1}{\delta^2}\ln\left(\frac{b-s+x}{2b}\right)\right] - (b+s-x)\left(1+\frac{1}{\delta^2 b}\right)}, \quad (6)$$

with

$$x = \sqrt{(s+b)^2 - 4\delta^2 s b^2/(1+\delta^2 b)}. \quad (7)$$

Here, the values of s and b were obtained by multiplying the total signal and SM background cross sections, respectively, by the integrated luminosity. δ is the percentage systematic error on the SM background estimate. In the limit of $\delta \to 0$, these expressions can be simplified as

$$\mathcal{Z}_{\text{disc}} = \sqrt{2[(s+b)\ln(1+s/b) - s]},$$
$$\mathcal{Z}_{\text{excl}} = \sqrt{2[s - b\ln(1+s/b)]}. \quad (8)$$

In this work we choose two cases: no systematics ($\delta = 0$) and a systematic uncertainty of $\delta = 10\%$.

TABLE II. Cut flow of the cross sections (in 10^{-3} fb) for the signals and SM backgrounds at the CLIC with $\kappa_B = 0.2$ and three typical B quark masses for the singlet case and doublet case (in the bracket).

	Signals			Backgrounds		
Cuts	1300 GeV	1500 GeV	2000 GeV	$\nu\bar{\nu}b\bar{b}$	$\nu\bar{\nu}jj$	Total
Basic	11 (44)	8.5 (38)	5.5 (22)	223590	50120	273710
Cut 1	8 (32)	7 (28)	4.1 (16.4)	128500	5359	133859
Cut 2	7.5 (30)	6.5 (26)	3.6 (14.4)	206	25	231
Cut 3	6.1 (24.4)	5.6 (22.4)	3.3 (13.2)	92	12	104

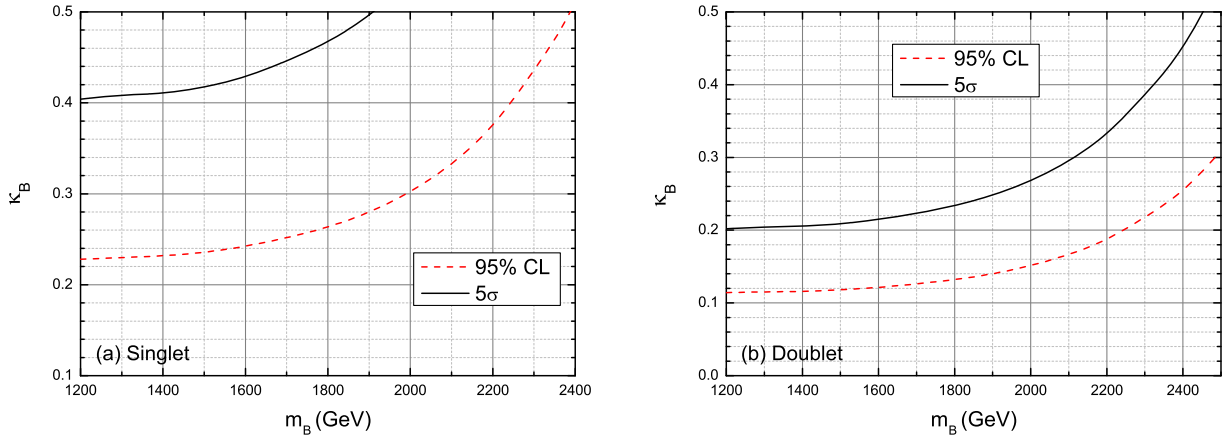

FIG. 5. The exclusion limit (at 95% CL) and discovery prospects (at 5σ) contour plots for the signal in $\kappa_B - m_B$ planes at 3 TeV CLIC with integral luminosity 5 ab^{-1} for $Z \to \ell^+\ell^-$ decay channel.

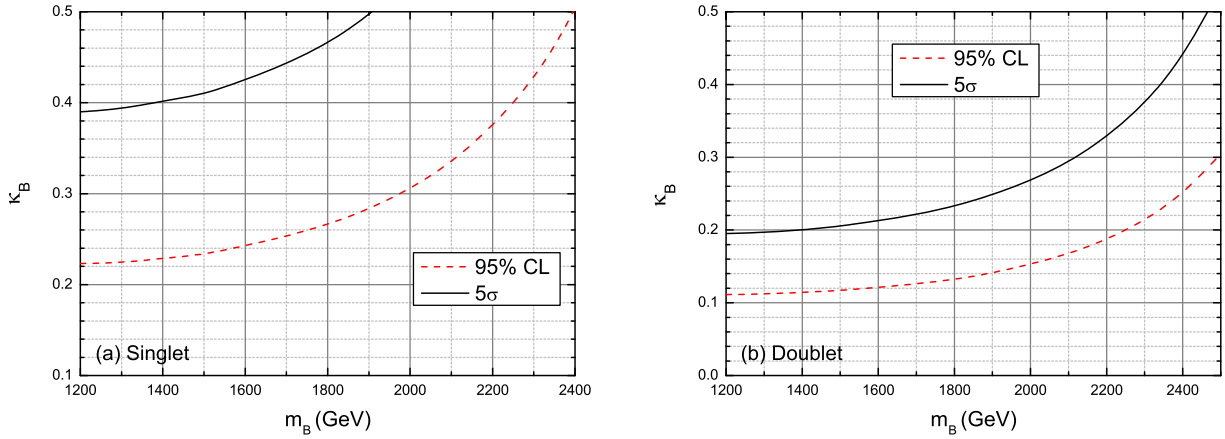

FIG. 6. Same as Fig. 5 but for $Z \to \nu\bar{\nu}$ decay channel.

In Figs. 5 and 6, we plot the exclusion limit at 95% confidence level (CL) and 5σ sensitivity reaches for the coupling strength κ_B as a function of m_B at 3 TeV CLIC with integral luminosity 5 ab^{-1}, respectively, for two decay channels without considering the effect of the systematic error. One finds that, for the $Z \to \ell^+\ell^-$ decay channel, the singlet (doublet) VLQ-B quarks can be excluded in the region of $\kappa_B \in [0.23, 0.62]([0.11, 0.31])$ and $m_B \in [1200\ \text{GeV}, 2500\ \text{GeV}]$ at the 3 TeV CLIC with the integrated luminosity of 5 ab^{-1}, while the discover region can reach $\kappa_B \in [0.4, 0.53]([0.2, 0.55])$ and $m_B \in [1200\ \text{GeV}, 2000\ \text{GeV}]$ ([1200 GeV, 2500 GeV]). Similarly, for $Z \to \nu\bar{\nu}$ decay channel, the singlet (doublet) VLQ-B quarks can be excluded in the region of $\kappa_B \in [0.22, 0.5]([0.11, 0.3])$ and $m_B \in [1200\ \text{GeV}, 2400\ \text{GeV}]$ ([1200 GeV, 2500 GeV]), the discover region can reach $\kappa_B \in [0.39, 0.5]([0.2, 0.44])$ and $m_B \in [1200\ \text{GeV}, 1900\ \text{GeV}]$ ([1200 GeV, 2400 GeV]).

Certainly, the sensitivities with some systematic errors will be weaker than those without any systematic error. Next, we combine the significance with $\mathcal{Z}_{\text{comb}} = \sqrt{\mathcal{Z}^2_{\ell\bar{\ell}} + \mathcal{Z}^2_{\nu\bar{\nu}}}$ by using the results from above two decay channels with the aforementioned two systematic error cases of $\delta = 0$ and $\delta = 10\%$.

In Fig. 7, the combined 95% CL exclusion limit and 5σ discovery prospect lines are drawn in $\kappa_B - m_B$ planes at the 3 TeV CLIC. One can see that, with a realistic 10% systematic error, the sensitivities are slightly weaker than those without any systematic error. For the singlet and doublet cases, the discovery region can, respectively, reach $\kappa_B \in [0.42, 0.52]$ with the VLQ-B mass range $m_B \in [1200\ \text{GeV}, 1900\ \text{GeV}]$, and $\kappa_B \in [0.21, 0.47]$ with the VLQ-B mass range $m_B \in [1200\ \text{GeV}, 2400\ \text{GeV}]$. Otherwise, in the region of $m_B \in [1200\ \text{GeV}, 2400\ \text{GeV}]$, the 95% CL excluded region for the coupling parameter κ_B is [0.23, 0.5] for the singlet case and [0.11, 0.25] for the doublet case, respectively, at the 3 TeV CLIC with an integrated luminosity of 5 ab^{-1}.

The ATLAS Collaboration has studied single production of a vectorlike B quark decaying into bH with $H \to \gamma\gamma$

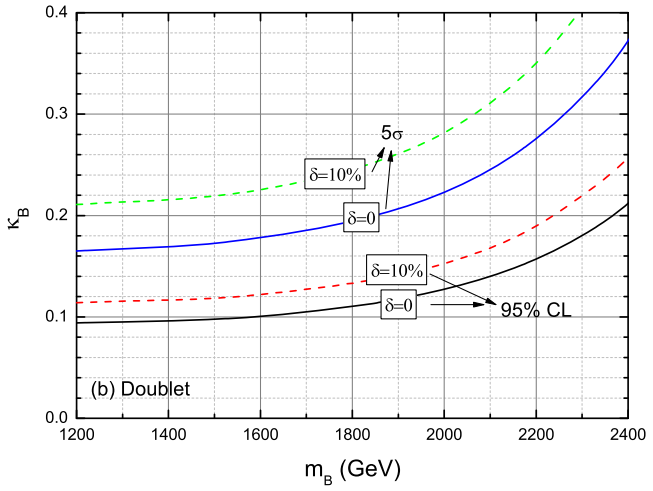

FIG. 7. Combined exclusion limit (at 95% CL) and discovery prospects (at 5σ) contour plots for the signal in $\kappa_B - m_B$ planes at 3 TeV CLIC with an integral luminosity of 5 ab^{-1} for the singlet (left) and doublet (right) cases.

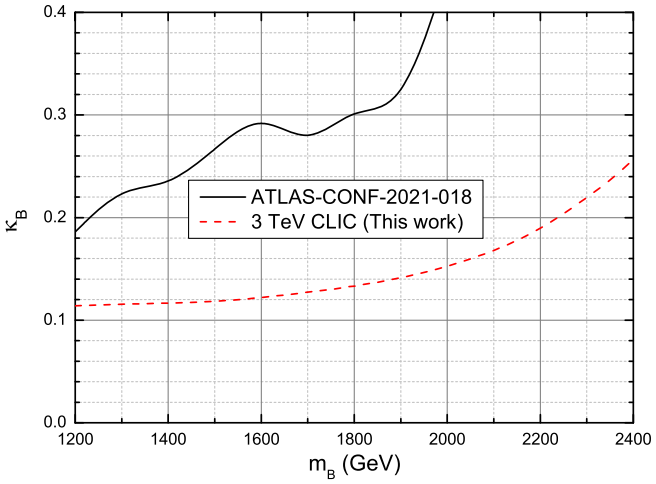

FIG. 8. The contour of 95% CL exclusion limit on the plane of m_B versus κ_B in the (B, Y) doublet scenarios with a realistic 10% systematic error. The solid line indicates the current expected limits from the LHC [76].

decay channel, assuming a generalized coupling $\kappa_B = 0.5$ and doublet branching ratios of 50% for $B \to hb$ and $B \to Zb$, B quark with masses less than 1210 GeV are excluded at the 95% CL [75]. Very recently, the ATLAS Collaboration has presented the limit from the single production of a VLQ-B occurring as part of a (B, Y) weak isospin doublet via $B \to bH(H \to b\bar{b})$ decay channel at 13 TeV LHC with 139 fb^{-1} luminosity, excluding $1.0\ \text{TeV} < m_B < 1.28\ \text{TeV}$ and $1.46\ \text{TeV} < m_B < 2.0\ \text{TeV}$ for $\kappa_B = 0.25$, and $1.0\ \text{TeV} < m_B < 2.0\ \text{TeV}$ for $\kappa_B = 0.3$ [76]. In Fig. 8, we give the current results at 13 TeV LHC and future reach at 3 TeV CLIC on the plane of m_B versus κ_B in the (B, Y) doublet scenarios. We can see that the future CLIC with $\sqrt{s} = 3$ TeV and integrated luminosity of 5 ab^{-1} could provide better sensitivity to detect the BbZ couplings than the current experimental results obtained from the current 13 TeV LHC. For high energy hadron colliders, the QCD backgrounds will be enhanced due to the pileup effect. By comparison, the properties of the VLQ-B can be measured accurately once it is discovered due to the clean SM backgrounds at the future leptonic colliders.

IV. CONCLUSION

We have studied single production of VLQ-B at the future 3 TeV CLIC via the process $e^+e^- \to B\bar{b} \to Zb\bar{b}$ in a model-independent way. We performed a full simulation for the signals and the relevant SM backgrounds based on two types of decay channels $Z \to \ell^+\ell^-$ $(\ell = e, \mu)$ and $Z \to \nu\bar{\nu}$. The 5σ discovery prospects and 95% CL exclusion limits in the parameter plane of the two variables m_B and κ_B were, respectively, obtained at 3 TeV CLIC with an integral luminosity of 5 ab^{-1}. Our numerical results show that, with the systematic error case of $\delta = 10\%$, in the region of $m_B \in [1200\ \text{GeV}, 2300\ \text{GeV}]$, the discovery region can reach $\kappa_B \in [0.42, 0.52]$ with the VLQ-B mass range $m_B \in [1200\ \text{GeV}, 1900\ \text{GeV}]$ for the singlet case, and $\kappa_B \in [0.21, 0.47]$ with the VLQ-B mass range $m_B \in [1200\ \text{GeV}, 2400\ \text{GeV}]$ for the doublet case, respectively. Otherwise, in the region of $m_B \in [1200\ \text{GeV}, 2400\ \text{GeV}]$, the excluded region for the coupling parameter κ_B is [0.23, 0.5] for the singlet case and [0.11, 0.25] for the doublet case, respectively, at the 3 TeV CLIC with an integrated luminosity of 5 ab^{-1}.

ACKNOWLEDGMENTS

The work is supported by the Foundation of the Henan Science and Technology Research Project No. 202102210223; Key Research Projects in Universities of Henan:21A140031; Henan Colleges and Universities Youth Teacher Training Project No. 2020GGJS212.

[1] A. De Simone, O. Matsedonskyi, R. Rattazzi, and A. Wulzer, J. High Energy Phys. 04 (2013) 004.
[2] N. Arkani-Hamed, A. G. Cohen, E. Katz, and A. E. Nelson, J. High Energy Phys. 07 (2002) 034.
[3] K. Agashe, G. Perez, and A. Soni, Phys. Rev. D **75**, 015002 (2007).
[4] K. Agashe, R. Contino, and A. Pomarol, Nucl. Phys. **B719**, 165 (2005).
[5] H. J. He, T. M. P. Tait, and C. P. Yuan, Phys. Rev. D **62**, 011702 (2000).
[6] X. F. Wang, C. Du, and H. J. He, Phys. Lett. B **723**, 314 (2013).
[7] H. J. He, C. T. Hill, and T. M. P. Tait, Phys. Rev. D **65**, 055006 (2002).
[8] H. J. He and Z. Z. Xianyu, J. Cosmol. Astropart. Phys. 10 (2014) 019.
[9] J. A. Aguilar-Saavedra, R. Benbrik, S. Heinemeyer, and M. Pérez-Victoria, Phys. Rev. D **88**, 094010 (2013).
[10] G. D. Kribs, T. Plehn, M. Spannowsky, and T. M. P. Tait, Phys. Rev. D **76**, 075016 (2007).
[11] S. Banerjee, M. Frank, and S. K. Rai, Phys. Rev. D **89**, 075005 (2014).
[12] M. Buchkremer, G. Cacciapaglia, A. Deandrea, and L. Panizzi, Nucl. Phys. **B876**, 376 (2013).
[13] D. Barducci and L. Panizzi, J. High Energy Phys. 12 (2017) 057.
[14] G. Cacciapaglia, A. Carvalho, A. Deandrea, T. Flacke, B. Fuks, D. Majumder, L. Panizzi, and H. S. Shao, Phys. Lett. B **793**, 206 (2019).
[15] B. Fuks and H. S. Shao, Eur. Phys. J. C **77**, 135 (2017).
[16] S. Yang, J. Jiang, Q. S. Yan, and X. Zhao, J. High Energy Phys. 09 (2014) 035.
[17] D. Liu, L. T. Wang, and K. P. Xie, J. High Energy Phys. 01 (2019) 157.
[18] G. Cacciapaglia, A. Deandrea, N. Gaur, D. Harada, Y. Okada, and L. Panizzi, J. High Energy Phys. 11 (2018) 055.
[19] J. A. Aguilar-Saavedra, J. Alonso-González, L. Merlo, and J. M. No, Phys. Rev. D **101**, 035015 (2020).
[20] D. Wang, L. Wu, and M. Zhang, Phys. Rev. D **103**, 115017 (2021).
[21] Y. J. Zhang, L. Han, and Y. B. Liu, Phys. Lett. B **768**, 241 (2017).
[22] L. Han, Y. J. Zhang, and Y. B. Liu, Phys. Lett. B **771**, 106 (2017).
[23] Y. B. Liu, Nucl. Phys. **B923**, 312 (2017).
[24] Y. B. Liu and Y. Q. Li, Eur. Phys. J. C **77**, 654 (2017).
[25] Y. B. Liu and S. Moretti, Phys. Rev. D **100**, 015025 (2019).
[26] X. Y. Tian, L. F. Du, and Y. B. Liu, Nucl. Phys. **B965**, 115358 (2021).
[27] S. Moretti, D. O'Brien, L. Panizzi, and H. Prager, Phys. Rev. D **96**, 075035 (2017).
[28] S. Moretti, D. O'Brien, L. Panizzi, and H. Prager, Phys. Rev. D **96**, 035033 (2017).
[29] A. Carvalho, S. Moretti, D. O'Brien, L. Panizzi, and H. Prager, Phys. Rev. D **98**, 015029 (2018).
[30] A. Roy, N. Nikiforou, N. Castro, and T. Andeen, Phys. Rev. D **101**, 115027 (2020).
[31] A. Buckley, J. M. Butterworth, L. Corpe, D. Huang, and P. Sun, SciPost Phys. **9**, 069 (2020).
[32] A. Deandrea, T. Flacke, B. Fuks, L. Panizzi, and H. S. Shao, J. High Energy Phys. 08 (2021) 107.
[33] S. J. D. King, S. F. King, S. Moretti, and S. J. Rowley, J. High Energy Phys. 05 (2021) 144.
[34] A. Atre, G. Azuelos, M. Carena, T. Han, E. Ozcan, J. Santiago, and G. Unel, J. High Energy Phys. 08 (2011) 080.
[35] M. Aaboud *et al.* (ATLAS Collaboration), Phys. Rev. D **98**, 092005 (2018).
[36] M. Aaboud *et al.* (ATLAS Collaboration), J. High Energy Phys. 12 (2018) 039.
[37] M. Aaboud *et al.* (ATLAS Collaboration), J. High Energy Phys. 08 (2018) 048.
[38] M. Aaboud *et al.* (ATLAS Collaboration), J. High Energy Phys. 05 (2019) 164.
[39] A. M. Sirunyan *et al.* (CMS Collaboration), Eur. Phys. J. C **79**, 364 (2019).
[40] A. M. Sirunyan *et al.* (CMS Collaboration), Phys. Rev. D **100**, 072001 (2019).
[41] A. M. Sirunyan *et al.* (CMS Collaboration), J. High Energy Phys. 08 (2018) 177.
[42] A. M. Sirunyan *et al.* (CMS Collaboration), Phys. Rev. D **102**, 112004 (2020).
[43] M. Aaboud *et al.* (ATLAS Collaboration), Phys. Rev. Lett. **121**, 211801 (2018).
[44] J. Nutter, R. Schwienhorst, D. G. E. Walker, and J. H. Yu, Phys. Rev. D **86**, 094006 (2012).
[45] X. Gong, C. X. Yue, and Y. C. Guo, Phys. Lett. B **793**, 175 (2019).
[46] X. Gong, C. X. Yue, H. M. Yu, and D. Li, Eur. Phys. J. C **80**, 876 (2020).
[47] H. Abramowicz *et al.* (CLIC Detector and Physics Study Collaborations), arXiv:1307.5288.
[48] J. de Blas, R. Franceschini, F. Riva, P. Roloff, U. Schnoor, M. Spannowsky, J. D. Wells, A. Wulzer, J. Zupan, S. Alipour-Fard *et al.*, CERN Yellow Rep. Monogr. **3**, 1 (2018).
[49] R. Franceschini, Int. J. Mod. Phys. A **35**, 2041015 (2020).
[50] D. Dannheim, P. Lebrun, L. Linssen, D. Schulte, and S. Stapnes, arXiv:1305.5766.
[51] R. Kitano, T. Moroi, and S. f. Su, J. High Energy Phys. 12 (2002) 011.
[52] K. Kong and S. C. Park, J. High Energy Phys. 08 (2007) 038.
[53] A. Senol, A. T. Tasci, and F. Ustabas, Nucl. Phys. **B851**, 289 (2011).
[54] K. Harigaya, S. Matsumoto, M. M. Nojiri, and K. Tobioka, J. High Energy Phys. 01 (2012) 135.
[55] A. B. Mahfoudh, L. Guo, W. Liu, W. G. Ma, R. Y. Zhang, and W. J. Zhang, Commun. Theor. Phys. **62**, 824 (2014).
[56] Y. B. Liu and Z. J. Xiao, Nucl. Phys. **B892**, 63 (2015).
[57] X. Qin and J. F. Shen, Nucl. Phys. **B966**, 115388 (2021).
[58] L. Han and J. F. Shen, Eur. Phys. J. C **81**, 463 (2021).
[59] A. Atre, M. Carena, T. Han, and J. Santiago, Phys. Rev. D **79**, 054018 (2009).
[60] For a comprehensive review, H. J. He, Y. P. Kuang, and C. P. Yuan, arXiv:hep-ph/9704276.
[61] H. J. He, Y. P. Kuang, and X. y. Li, Phys. Rev. Lett. **69**, 2619 (1992).

[62] H. J. He, Y. P. Kuang, and X. y. Li, Phys. Rev. D **49**, 4842 (1994).
[63] H. J. He, Y. P. Kuang, and C. P. Yuan, Phys. Rev. D **51**, 6463 (1995).
[64] H. J. He, Y. P. Kuang, and C. P. Yuan, Phys. Rev. D **55**, 3038 (1997).
[65] H. J. He and W. B. Kilgore, Phys. Rev. D **55**, 1515 (1997).
[66] J. Alwall, R. Frederix, S. Frixione, V. Hirschi, F. Maltoni, O. Mattelaer, H.-S. Shao, T. Stelzer, P. Torrielli, and M. Zaro, J. High Energy Phys. 07 (2014) 079.
[67] M. Tanabashi *et al.* (Particle Data Group), Phys. Rev. D **98**, 030001 (2018).
[68] T. Sjöstrand, S. Ask, J. R. Christiansen, R. Corke, N. Desai, P. Ilten, S. Mrenna, S. Prestel, C. O. Rasmussen, and P. Z. Skands, Comput. Phys. Commun. **191**, 159 (2015).
[69] J. de Favereau, C. Delaere, P. Demin, A. Giammanco, V. Lemaître, A. Mertens, and M. Selvaggi (DELPHES 3 Collaboration), J. High Energy Phys. 02 (2014) 057.
[70] E. Leogrande, P. Roloff, U. Schnoor, and M. Weber, arXiv: 1909.12728.
[71] M. Boronat, J. Fuster, I. Garcia, E. Ros, and M. Vos, Phys. Lett. B **750**, 95 (2015).
[72] M. Boronat, J. Fuster, I. Garcia, P. Roloff, R. Simoniello, and M. Vos, Eur. Phys. J. C **78**, 144 (2018).
[73] E. Conte, B. Fuks, and G. Serret, Comput. Phys. Commun. **184**, 222 (2013).
[74] G. Cowan, K. Cranmer, E. Gross, and O. Vitells, Eur. Phys. J. C **71**, 1554 (2011); **73**, 2501(E) (2013).
[75] ATLAS Collaboration, ATLAS-CONF-2018-024.
[76] ATLAS Collaboration, ATLAS-CONF-2021-018.